

# Fabrication of floated graphite/graphene based composite counter electrode for dye-sensitized solar cell

A. A. B. Madushani<sup>1</sup>, P. Kumarasinghe<sup>2</sup>, G.R.A. Kumara<sup>2</sup>, L.R.A.K. Bandara<sup>3</sup>,

<sup>1</sup> Postgraduate Institute of Science, University of Peradeniya, Peradeniya, Sri Lanka

<sup>2</sup> National Institute of Fundamental Studies, Hantana road, Kandy, Sri Lanka

<sup>3</sup> Department of Physics, Faculty of Science, University of Peradeniya, Peradeniya, Sri Lanka.

\*\*\*

**Abstract** - Dye-sensitized Solar Cells are gaining much attention as an alternative to silicon-based solar cells due to their low cost, easy fabrication and reasonable efficiency. Platinum is still widely used as a counter electrode material in DSC devices. In this research, highly expensive Pt counter electrode has been replaced by low cost floated graphite/graphene composite CE. The composite counter electrode was developed on conducting glass substrate by screen printing method. Graphene and floated graphite were prepared using Sri Lankan natural vein graphite where modified Hummer's method used for the preparation of graphene. Power conversion efficiency was optimized by varying graphene/graphite composition and thickness of the composite film. A maximum power conversion efficiency of 5.88% showed the DSC fabricated using composite counter electrode with 1:1 graphene/graphite ratio, which is comparable to 8.24% of Pt counter electrode based solar cell.

**Key Words:** Dye-sensitized Solar Cells, Fabrication, graphene, screen-printed composite material

catalytic layer in CEs due to its good conductivity and low cost [5-8]. Among them carbon-based materials stand out to be the best alternative as far as low-cost and ready abundance are concerned. One disadvantage of carbon CE-based DSCs is that carbon has considerably inferior catalytic activity for triiodide reduction when compared to that of platinum thus limiting the solar cell efficiencies towards much lower values when compared to those of Pt-CE based DSCs. However, carbon based CEs are inexpensive, non-toxic and reduce iodine corrosion than Pt CE. Commonly used carbon materials are, carbon black [9], activated charcoal [10-13], carbon nanotubes [14, 15], graphite [16, 17] and graphene [18]. Vein graphite is a low-cost material which is readily available in Sri Lanka. In this research, it has been developed a low-cost floated graphite and graphene composite counter electrode for DSC. Floated graphite/graphene layer was deposited on fluorine-doped tin oxide (FTO) glass substrate by screen printed method. Hummer's method was used for synthesizing graphene from Sri Lankan vein graphite. This composite counter electrode was optimized by changing the mixing ratio of floated graphite and graphene and thickness of the composite layer.

## 1. INTRODUCTION

Dye-sensitized solar cells (DSCs) are low-cost alternatives to silicon solar cells and the breakthrough was done by Gratzel and O'Regan in 1991 reporting efficiencies over 7% [1]. Numerous research in DSC have enhanced and innumerable modifications done have resulted in efficiencies closer to 15% [2]. Current studies on DSCs mainly focus on fabricating low-cost cell with high performances. The basic structure of sandwich type of DSC consists of transparent conducting oxide (TCO) electrode/ meso-porous TiO<sub>2</sub> layer/ dye/ electrolyte/ counter electrode (CE). The CE assists electron transmission from the outer circuit to the redox electrolyte. The catalytic layer in CE material is essential for the reduction of I<sup>-</sup>/ I<sub>3</sub><sup>-</sup> in the electrolyte [3-4]. Cost of DSCs depends mainly on the counter electrode (CE) material where the best catalyst for triiodide reduction at the CE is platinum (Pt), which is highly expensive. Thus the development of DSCs required finding low-cost CE materials with good catalytic activity and high electrical conductivity. Recently different forms of carbonaceous materials, inorganic materials and polymers have been examined as a

## 2. MATERIAL AND METHODS

### 2.1 Preparation of Graphene

According to the modified hummers method first, ball milled graphite (particle size <45 μm) (1 g) (99%, Bogala) was added to Conc.H<sub>2</sub>SO<sub>4</sub> acid (50ml) (98%, Merck) while stirring in an ice-water bath. Then, KMnO<sub>4</sub> (3 g) (Sigma Aldrich) was gradually added by maintaining the temperature under 10 °C. Then, the solution was stirred at room temperature for 25 minutes followed by 5 minutes sonication in an ultrasonic bath. The stirring-sonication process was repeated for 12 times, 200 ml of distilled water was added an extra 2 hours ultrasonic treatment was carried out. Then, 1M NaOH solution (>98%, Sigma Aldrich) was added to adjust the pH at ~ 6 and the solution was sonicated for 1 hour. Then, 20 g L-ascorbic acid (Sigma Aldrich) was dissolved in 200 ml distilled water and then the mixture was slowly added to the exfoliated graphite oxide suspension at room temperature. After that, the solution was heated to 95 °C for 1 hour. Then, resultant black precipitates were simply filtered by cellulose filter paper and further was washed with a 1M HCl acid

solution (37%, Merck) and distilled water to neutral pH. Finally, the filtrate was freeze-dried to obtain graphene powder.

## 2.2 Preparation of floated graphite

Ball milled graphite (particle size  $<45\ \mu\text{m}$ ) (99%, Bogala) was added to a water beaker. Then it was boiled using a Bunsen burner and floated graphite on the water surface was collected using a glass strip to a small beaker. Then it was heated up to  $100\ ^\circ\text{C}$  to evaporate excess water to get the floated graphite powder.

## 2.3 Preparation of floated graphite/graphene composite counter paste

The composite paste was prepared using a mixture of floated graphite, graphene and an organic binder, cellulose methyl carboxylate (CMC). First, graphene 0.100 g, floated graphite 0.100 g, distilled water 8 ml, ethanol 4 ml and carboxylic methyl cellulose (CMC) 0.025 g were ground well in a mortar. Then the mixture was kept on a hot plate at  $80\ ^\circ\text{C}$  to evaporate excess water and ethanol until a composite paste is obtained.

## 2.4 Fabrication of the composite film

The cleaned FTO glass plate was tightly fixed on the basement using double side tapes. The conducting side of the glass plate should be in upward. Then the screen was fixed on the basement in such a way that selected mesh was right over the glass plate. Here care should be taken to avoid contact between mesh and the glass plate. Then, a small portion of the composite paste was laid on the upper edge of the selected mesh. Finally, the composite paste was uniformly spread over the mesh using a scraper and composite layer was printed on the conducting side of the glass plate.

After applying the first layer, the substrate was kept on a hot plate at  $100\ ^\circ\text{C}$  for 10 minutes to dry. Then again repeat the above procedure and another layer was printed. This procedure was repeated until the desired thickness is obtained. After applying the final layer the glass plate was sintered at  $300\ ^\circ\text{C}$  for 30 minutes. To obtain the optimized mixing ratios of floated graphite, graphene was changed as 1:0, 1:1, 1:2, 2:1, 0:1 with a total weight of 0.200 g and counter electrodes were prepared.

## 2.5 Preparation of $\text{TiO}_2$ working electrode

The  $\text{TiO}_2$  colloidal solution was prepared using titanium tetraisopropoxide (20.0 ml) and acetic acid (2.5 ml) mixing with ethanol (25.0 ml). Then, steam was passed through the solution until a gel type transparent  $\text{TiO}_2$  colloidal formed. After that,  $\text{TiO}_2$  colloid was grounded with distilled water (50.0 ml) in a mortar and autoclaved for three hours at  $150\ ^\circ\text{C}$ . The precursor solution was made by 20.0 ml of  $\text{TiO}_2$  colloidal solution, 5.5 ml of acetic acid, 20 ml of ethanol and 5

drops of triton X-100, then ultra-sonicated for 10 minutes. Conductive FTO glass plates ( $1\times 2\ \text{cm}^2$ ) were cleaned with detergents and then ultra-sonicated for 10 minutes in distilled water, before used. To fabrication of  $\text{TiO}_2$  film, half area ( $1\times 1\ \text{cm}^2$ ) of the conducting side of the FTO glasses were covered with aluminium foil and placed on a pre-heated ( $150\ ^\circ\text{C}$ ) hot plate. Then the above prepared solution was sprayed by hand spray method and finally sintered at  $500\ ^\circ\text{C}$  in a furnace for 30 minutes.

## 2.6 Dye adsorption process

The  $\text{TiO}_2$  coated FTO glasses that pre-heated to  $80\ ^\circ\text{C}$  were immersed in a mixture of acetonitrile/tetra-butyl alcohol 1:1 by volume containing 0.3 M Ruthenium N-719, for 12 hours. After that, the electrodes were taken out and were washed with acetonitrile to remove the excess dye molecules.

## 2.7 Fabrication of Solar cell device

In this research, the dye-sensitized solar cells were fabricated using the N719 dye-coated working electrode and screen printed floated graphite/graphene composite counter electrode. The working electrode and counter electrode were assembled by sandwiching the electrolyte (0.1 M LiI, 0.05 M  $I_2$ , 0.6 M dimethylpropylimidazolium iodide in methoxyacetonitrile) with  $I^-/I_3^-$  as the redox couple. The current density-voltage (J-V) measurements of the DSCs were recorded at AM 1.5 ( $100\ \text{mW cm}^{-2}$ ) simulated sunlight radiation system (PE Cell-PEC L- 01)

## 3. RESULTS AND DISCUSSION

### 3.1 Optimization of the film thickness of the composite counter electrode for different compositions of floated graphite and graphene

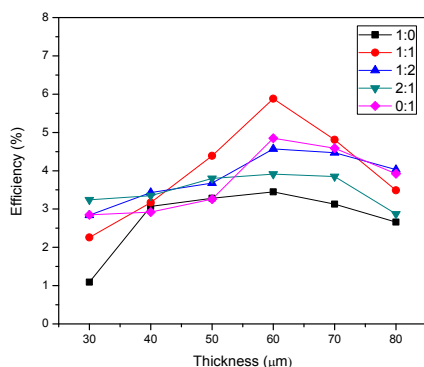
The sintering temperature and Carboxyl methyl cellulose (CMC) amounts were kept constant, and thickness of the film was varied, to find the optimum film thickness for different floated graphite, graphene ratios as 1:0, 1:1, 1:2, 2:1 and 0:1. To find the optimum thickness, the film thickness was varied by applying several layers of composite pastes onto the FTO glass plate using screen printing technique. Finally, the thickness was measured using a digital micrometre. Table 1 depicts the photovoltaic measurements for DSCs with counter electrodes using floated graphite: graphene in 1:1 ratio. The thickness was changed from  $30\ \mu\text{m}$  to  $60\ \mu\text{m}$ . The thickness cannot be increased beyond  $80\ \mu\text{m}$  without having cracks. The table shows the highest efficiency of 5.88% for  $60\ \mu\text{m}$  thick composite layer. The open circuit voltage (VOC) and short circuit current (JSC) were increased with the thickness up to  $60\ \mu\text{m}$ , and then it was decreased. The above data confirmed that the efficiency of a solar cell depends on the thickness of the composite layer. The highest conversion efficiency,  $\eta=5.88\%$  was achieved at the thickness of  $60\ \mu\text{m}$  with JSC of  $12.05\ \text{mA cm}^{-2}$ , VOC of  $740$

mV and fill factor 66%. Up to 60 μm the efficiency of the solar cell increased due to defects and functional groups at the edge planes of the graphene layers. Because of that, the catalytic activity of the cell improved with thickness up to 60 μm.

**Table - 1:** Photovoltaic parameters of DSCs using floated graphite: graphene in 1:1 ratio counter electrodes fabricated in different thickness

Approximate Thickness/ μm	$V_{oc}$ / V	$J_{sc}$ / mA cm <sup>-2</sup>	FF	Efficiency/ %
30	0.562	9.40	0.43	2.26
40	0.646	9.60	0.51	3.17
50	0.683	10.74	0.60	4.39
60	0.740	12.05	0.66	5.88
70	0.754	10.31	0.62	4.81
80	0.650	8.57	0.63	3.49

For the determination of the performance of a solar cell, the charge transfer resistance ( $R_{CT}$ ) and sheet resistance ( $R_s$ ) of the counter electrode are important factors since they have a negative effect on energy conversion. It is obvious that for a thick film of counter electrodes, the charge transfer resistance is lower than for thin layers and this directly affects the fill factor (FF) and charge transfer resistance ( $R_{CT}$ ) [19, 20]. According to the Table 1 at higher thicknesses the fill factors are higher than for lower thicknesses. Further, the short circuit current density ( $J_{sc}$ ), increased until an optimum thickness and thereafter it dropped. This can be explained by the effect of sheet resistance. As thickness increased further, the sheet resistance became prominent and starts to affect the short circuit current and reduced the cell performance.



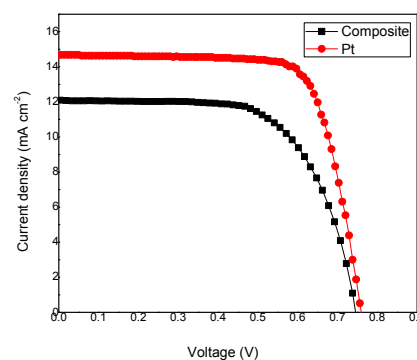
**Fig - 1:** Variation of efficiency with film thickness for the sample with different floated graphite: graphene ratios.

Figure 1 shows the variation of efficiency for five mixing ratios of floated graphite: graphene with the thickness of the film. For all compositions, the maximum efficiency observed

for 60μm thickness and the performance of the cells were maximum at that thickness. At the thickness of 60 μm the maximum efficiency 5.88% was obtained for 1:1 composition, the second maximum efficiency 4.85% was obtained for 0:1 composition counter electrode, then the third maximum efficiency 4.57% was obtained for 1:2 composition counter electrode, the fourth maximum efficiency 3.96% was obtained for 2:1 composition counter electrode and the lowest efficiency 3.45% was obtained for 1:0 counter electrode. Graphite has poor catalytic activity than graphene towards the reduction of  $I_3^-$ . Increasing graphene amount of composite counter electrode, the efficiency of the solar cell improved except for the 1:1 composition counter electrode.

**3.2 I-V characteristics comparison of DSCs made from floated graphite: graphene 1:1 composition counter electrode and platinum counter electrodes**

Platinum has high catalytic activity toward  $I_3^-$  reduction and is sufficiently corrosion resistant to iodine species present in the electrolyte. Graphene is corrosion resistive, electrically conductive and has high catalytic activity. But, graphite has poor catalytic activity toward the reduction of  $I_3^-$ . It was found that the film thickness of the composite counter electrodes influences to the performance of the solar cell. When the thickness of the composite film increased, the catalytic active sites in the film increased. Due to that, the efficiency of the cell increases with the thickness. After reaching the optimum thickness, the efficiency of the cell decrease with the thickness. As further increasing the thickness, electrons need to travel more distance to reach the CE/electrolyte surface. This would increase the resistance for the mobility of electron with thickness and reduce efficiency. However, Pt counter electrodes require a very thin (few nanometers) layer for the catalytic activity in DSCs.



**Fig - 2:** The I-V Plots for DSCs fabricated with Pt and 1:1 composite counter electrodes

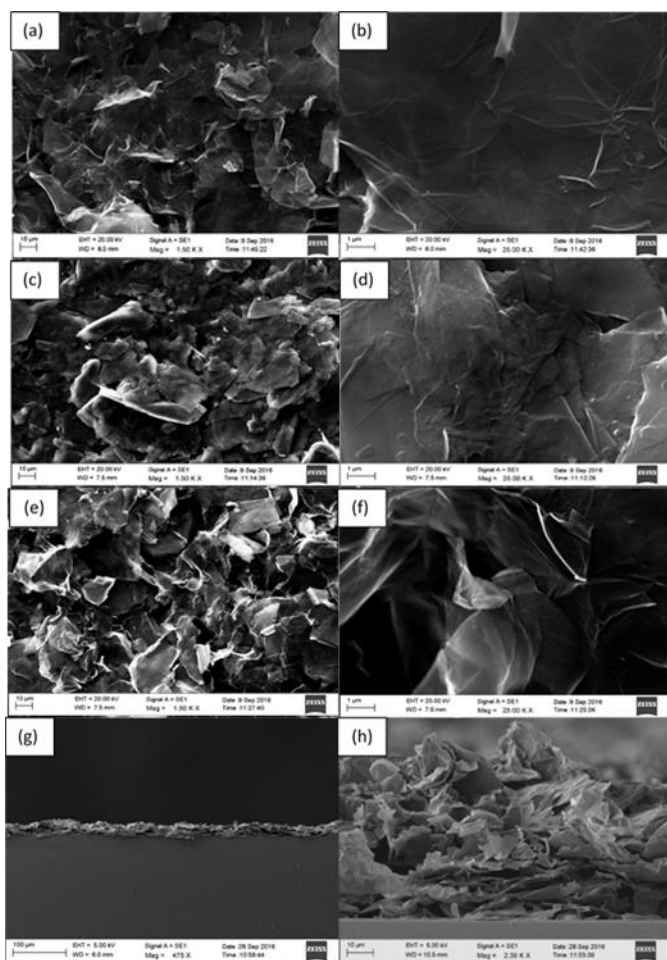
The J-V characteristics of the DSCs with Pt and 1:1 composite counter electrodes are shown in Figure 2. Composite counter electrode based DSC and Pt counter electrode based counter electrode shows a  $J_{sc}$  of 12.05 mA cm<sup>-2</sup>,  $V_{oc}$  of 0.740 mV, FF of 0.66 and  $J_{sc}$  of 14.67

mA cm<sup>-2</sup>, VOC of 0.759 mV, FF of 0.74 respectively. Pt based DSC showed the high efficiency of 8.24% than the composite counter electrode based DSC which shows 5.88% power conversion efficiency. Due to the low JSC, VOC and FF values, the DSCs with composite counter electrodes show low power conversion efficiency. This research implies the ability to substitute expensive platinum counter electrode by inexpensive graphene-floated graphite composite counter electrode that prepared using Sri Lankan vein graphite for DSCs.

affords to ultrathin and homogeneous graphene films. Figure 3 (c) and (d) show SEM images of the graphite counter electrode. It is clear that graphite counter electrode has small flakes and nonhomogeneous surface compared to graphene counter electrode. Figure 3 (e) and (f) show the SEM images of the composite counter electrode. The composite layer forms an open layered structure with pores on the micrometre scale. Three different magnification levels of SEM images shown in figure 3 (b), (d), and (f) clearly indicated the differences of the surface morphologies of graphene, graphite and composite counter electrodes. Figure 3 (f) shows the highly porous nature of the composite film which contributed to increase the surface area of the film. Figure 3 (g) and (h) are shown the cross section images of the composite counter electrode that pointing out layers are stack with each other.

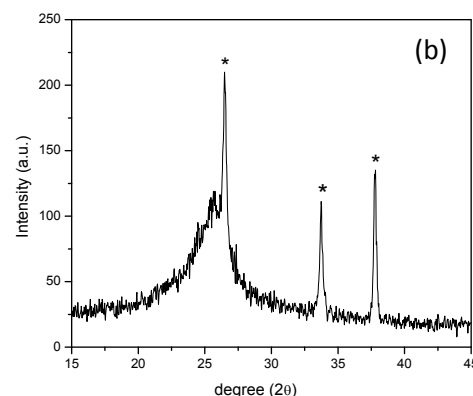
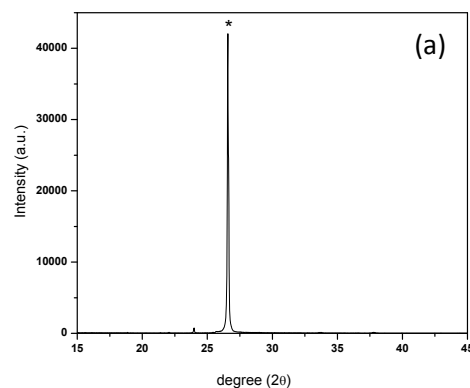
### 3.4 XRD analysis for the counter electrodes

The crystal structures of graphite, graphene and composite thin films were analyzed using X-ray diffraction. Siemens D5000 Powder X-Ray diffractometer was used to take the XRD spectrums. The measurements were taken in the range of 15° ≤ 2θ ≤ 45° using Cu Kα-radiation of wavelength λ=1.54 nm.



**Fig - 3:** SEM images of the surface of the graphene counter electrode with different magnifications (a), (b); floated graphite counter electrode with different magnifications (c), (d); 1:1 composition composite counter electrode with different magnifications (e), (f); cross section view of the SEM of the composite counter electrode at different magnification levels (g), (h).

Scanning electron microscopy (SEM) offers morphology and structure of materials. Figure 3 shows two magnification levels of SEM images. Figure 3 (a) and 3 (b) show the surface of the graphene counter electrode. The figures depict that graphene counter electrode has a layered structure, which



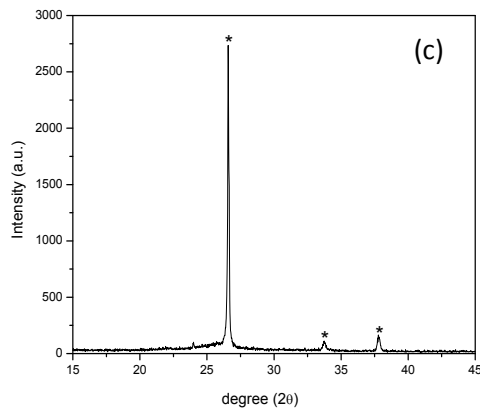


**Fig - 4:** (a), (b) and (c) XRD spectra for fabricated graphite, graphene and composite counter electrode.

The XRD pattern observed for graphite film screen printed on a FTO glass plate is shown in figure 4(a). It shows the diffraction peak at  $2\theta = 26.6^\circ$  for interlayer distance  $\sim 3.35 \text{ \AA}$  in (002) orientation. The XRD pattern for graphene based counter electrode is shown in Figure 4(b). The peaks which marked with stars belong to the (110), (101), and (200) peaks of the FTO pattern. The diffraction peak for graphene film can be observed around  $2\theta = 25.8^\circ$  with average interlayer distance  $\sim 3.45 \text{ \AA}$  in (002) orientation. Figure 4(a) And Figure 4(b) indicate there is a significant shift in the peak position of graphene and graphite films along (002) orientation due to the d space changing from  $3.35 \text{ \AA}$  to  $3.45 \text{ \AA}$ . Figure 4(c) is shown the XRD of the composite film. The diffraction peak was found around  $2\theta = 26.6^\circ$  for the average interlayer distance  $\sim 3.35 \text{ \AA}$  in (002) orientation.

#### 4. Conclusion

In this research, a successful method was introduced to fabricate floated graphite/graphene composite counter electrode for DSC using a purposely built screen printing technology. Hummers method was used to synthesis graphene from Sri Lankan vein graphite over 98% purity. The composite films were optimized in two aspects, the composition of the films and the thickness of the films. According to this optimization, it was found that the highest efficiency was achieved at a weight ratio of floated graphite to graphene 1:1, and a thickness of nearly  $60 \text{ \mu m}$ . Due to the formation of cracks, the thickness of the film cannot be raised beyond  $80 \text{ \mu m}$ . SEM images of the graphene film, graphite film, and 1:1 composite film was illustrated that the porous nature of the 1:1 composition counter electrode highly affected the efficiency of the DSC. The exfoliation of graphene sheets and the interlayer distance were confirmed by the XRD spectrums. Also, the best performance of the 1:1 composition counter electrode was comparable with the values of Pt. Therefore, for 1:1 composition counter

electrode, the maximum conversion efficiency of 5.88% was obtained whereas for Pt a value of 8.24% was obtained.

#### ACKNOWLEDGEMENT

The authors would like to thank the National Institute of Fundamental Studies, Sri Lanka for financial support.

#### REFERENCES

- [1] O'regan, B., & Grätzel, M. (1991). A low-cost, high-efficiency solar cell based on dye-sensitized colloidal TiO<sub>2</sub> films. *nature*, 353(6346), 737.
- [2] Kakiage, K., Aoyama, Y., Yano, T., Oya, K., Fujisawa, J. I., & Hanaya, M. (2015). Highly-efficient dye-sensitized solar cells with collaborative sensitization by silyl-anchor and carboxy-anchor dyes. *Chemical Communications*, 51(88), 15894-15897.
- [3] Kay, A., Grätzel, M., *Sol. Energ. Mat. Sol. C.* 1996, 44, 99-117.
- [4] Wroblowa, H.S., Saunders. A., *Electroanal. Chem. Int. Electrochem.* 1973, 42, 329.
- [5] S.S. Khalili, H. Dehghani, M. Afrooz, Composite films of metal doped CoS/carbon allotropes; efficient electrocatalyst counter electrodes for high performance quantum dot-sensitized solar cells, *J. Colloid Interface Sci.* 493 (2017) 32–41. doi:10.1016/j.jcis.2017.01.005.
- [6] M. Wu, T. Ma, Platinum-free catalysts as counter electrodes in dye-sensitized solar cells, *ChemSusChem.* 5 (2012) 1343–1357. doi:10.1002/cssc.201100676.
- [7] A. Ramachandran, I. Jinchu, C.O. Sreekala, Studies on polymer based counter electrodes for DSSC application, in: 2016 Int. Conf. Electr. Electron. Optim. Tech., IEEE, 2016: pp. 4628–4630. doi:10.1109/ICEEOT.2016.7755595.
- [8] P. Veerender, V. Saxena, A. Gusain, P. Jha, S.P. Koiry, A.K. Chauhan, D.K. Aswal, S.K. Gupta, Conducting polymers based counter electrodes for dye-sensitized solar cells, in: 2014: pp. 1048–1050. doi:10.1063/1.4872848.
- [9] T.N. Murakami, S. Ito, Q. Wang, M.K. Nazeeruddin, T. Bessho, I. Cesar, P. Liska, R. Humphry-Baker, P. Comte, P. Péchy, M. Grätzel, Highly Efficient Dye-Sensitized Solar Cells Based on Carbon Black Counter Electrodes, *J. Electrochem. Soc.* 153 (2006) A2255. doi:10.1149/1.2358087.
- [10] R. Kumar, S.S. Nemala, S. Mallick, P. Bhargava, Synthesis and characterization of carbon based counter electrode for dye sensitized solar cells (DSSCs) using sugar free as a carbon material, *Sol. Energy.* 144 (2017) 215–220. doi:10.1016/j.solener.2017.01.030.
- [11] Z. Xie, W. Guan, F. Ji, Z. Song, Y. Zhao, Production of Biologically Activated Carbon from Orange Peel and

- Landfill Leachate Subsequent Treatment Technology, *J. Chem.* 2014 (2014) 1–9. doi:10.1155/2014/491912.
- [12] R. Madhu, V. Veeramani, S.-M. Chen, J. Palanisamy, A.T. Ezhil Vilian, Pumpkin stem-derived activated carbons as counter electrodes for dye-sensitized solar cells, *RSC Adv.* 4 (2014) 63917–63921. doi:10.1039/C4RA12585A.
- [13] K.D.M.S.P.K. Kumarasinghe, G.R.A. Kumara, R.M.G. Rajapakse, D.N. Liyanage, K. Tennakone, Activated coconut shell charcoal based counter electrode for dye-sensitized solar cells, *Org. Electron. Physics, Mater. Appl.* 71 (2019) 93–97. doi:10.1016/j.orgel.2019.05.009.
- [14] S. Huang, H. Sun, X. Huang, Q. Zhang, D. Li, Y. Luo, Q. Meng, Carbon nanotube counter electrode for high-efficient fibrous dye-sensitized solar cells., *Nanoscale Res. Lett.* 7 (2012) 222. doi:10.1186/1556-276X-7-222.
- [15] J.G. Nam, Y.J. Park, B.S. Kim, J.S. Lee, Enhancement of the efficiency of dye-sensitized solar cell by utilizing carbon nanotube counter electrode, *Scr. Mater.* 62 (2010) 148–150. doi:10.1016/j.scriptamat.2009.10.008.
- [16] E.N. Jayaweera, G.R.A. Kumara, H.M.G.T.A. Pitawala, R.M.G. Rajapakse, N. Gunawardhana, H.M.N. Bandara, A. Senarathne, C.S.K. Ranasinghe, H.-H. Huang, M. Yoshimura, Vein graphite-based counter electrodes for dye-sensitized solar cells, *J. Photochem. Photobiol. A Chem.* 344 (2017) 78–83. doi:10.1016/j.jphotochem.2017.05.009.
- [17] Y.-Y. Li, C.-T. Li, M.-H. Yeh, K.-C. Huang, P.-W. Chen, R. Vittal, K.-C. Ho, Graphite with Different Structures as Catalysts for Counter Electrodes in Dye-sensitized Solar Cells, *Electrochim. Acta.* 179 (2015) 211–219. doi:10.1016/j.electacta.2015.06.007.
- [18] H. Wang, Y.H. Hu, Graphene as a counter electrode material for dye-sensitized solar cells, *Energy Environ. Sci.* 5 (2012) 8182. doi:10.1039/c2ee21905k.